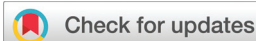


## RESEARCH ARTICLE

View Article Online  
View Journal | View IssueCite this: *Org. Chem. Front.*, 2024, **11**, 4408Site-specific DNA post-synthetic modification *via* fast photocatalytic allylation†Ying Huang,<sup>‡,a</sup> Yixin Zhang,<sup>‡,a</sup> Chenchen Hu<sup>a</sup> and Yiyun Chen<sup>\*,a,b,c</sup>

Expanding DNA functionality has significant implications in nucleic acid chemistry, biology, and beyond. Therefore, developing new chemical tools for site-specific post-synthetic modification of nucleic acids is urgently needed. Herein, we demonstrate the first site-specific DNA post-synthetic modification *via* visible-light-catalyzed decarboxylative allylation. Allyl sulfone groups were introduced into DNA, not only at the terminal sites *via* amide formation but also at internal and terminal positions during DNA solid-phase synthesis. This visible-light-catalyzed decarboxylative allylation proceeds rapidly on DNA bearing allyl sulfone groups under open-air conditions within minutes, exhibiting excellent chemoselectivity and compatibility with various functional groups while retaining DNA integrity. Specifically, introducing allyl sulfones into DNA *via* solid-phase synthesis enables site-specific modification on chemically synthesized single-stranded DNA (internal and terminal positions), hybridized double-stranded DNA, and enzymatically amplified long-chain DNA under visible light irradiation. The versatile reactivity of allyl sulfone scaffolds further enables diverse on-DNA photocatalytic transformations, promising to advance the chemical toolbox for DNA post-synthetic modification through diverse photochemical methods.

Received 25th April 2024,  
Accepted 16th June 2024

DOI: 10.1039/d4qo00752b

rsc.li/frontiers-organic

## Introduction

The post-synthetic modification of nucleic acids substantially expands their functionality. By precise modification *via* proper chemical reactions, the resulting functional nucleic acid with desired structures, properties, and functions offers promising opportunities for biological function probing, biosensing, drug delivery, nanozyme catalysis, drug screening, and beyond.<sup>1</sup> A recent example is the nucleoside modification contributes to developing effective mRNA vaccines, a discovery recognized by the 2023 Nobel Prize.<sup>2</sup> In the past decade, bioorthogonal reactions like copper-catalyzed azide–alkyne cycloaddition, strain-promoted azide–alkyne cycloadditions, and inverse-electron-demand Diels–Alder reactions have been extensively utilized for site-specific oligonucleotide modification with functional agents while preserving DNA integrity

for assembly and recognition.<sup>3</sup> Despite the remarkable advance in bioorthogonal chemistry for protein and carbohydrate bioconjugation, achieving precise post-synthetic modification of nucleic acids is different and remains a significant challenge.<sup>4</sup> In the chemical preparation of nucleic acids, nucleobases with specific reactive functional groups are typically synthesized first as DNA building blocks. This allows the incorporation of single or just a few functional groups at arbitrary positions during subsequent DNA synthesis, without affecting standard base pairing (Scheme 1a). These DNA building blocks bearing bioorthogonal reactive groups must withstand the harsh chemical conditions of the automated solid-phase DNA synthesis, including exposure to strong acids, bases, and oxidizers.<sup>5</sup> However, stability requirements may conflict with desired reactivity, impacting subsequent labeling reaction efficiency. Additionally, ensuring high selectivity and sufficient reactivity of the reaction groups in mild aqueous conditions during on-DNA transformation, while preserving DNA integrity, further complicates the realization of site-specific nucleic acid modification. Given these constraints, exploring and investigating novel chemical toolboxes for DNA modification is still in urgent demand.

Recent developments in photocatalysis offer a promising opportunity for mild, aqueous, and visible light-induced on-DNA transformation, primarily by producing alkyl radicals (Scheme 1b).<sup>6–8</sup> Photocatalysis has already demonstrated its significance in DNA-encoded library (DEL) technologies by enabling the rapid construction of diverse chemical structures

<sup>a</sup>State Key Laboratory of Chemical Biology, Shanghai Institute of Organic Chemistry, University of Chinese Academy of Sciences, Chinese Academy of Sciences, 345 Lingling Road, Shanghai 200032, P. R. China. E-mail: yiyunchen@sioc.ac.cn

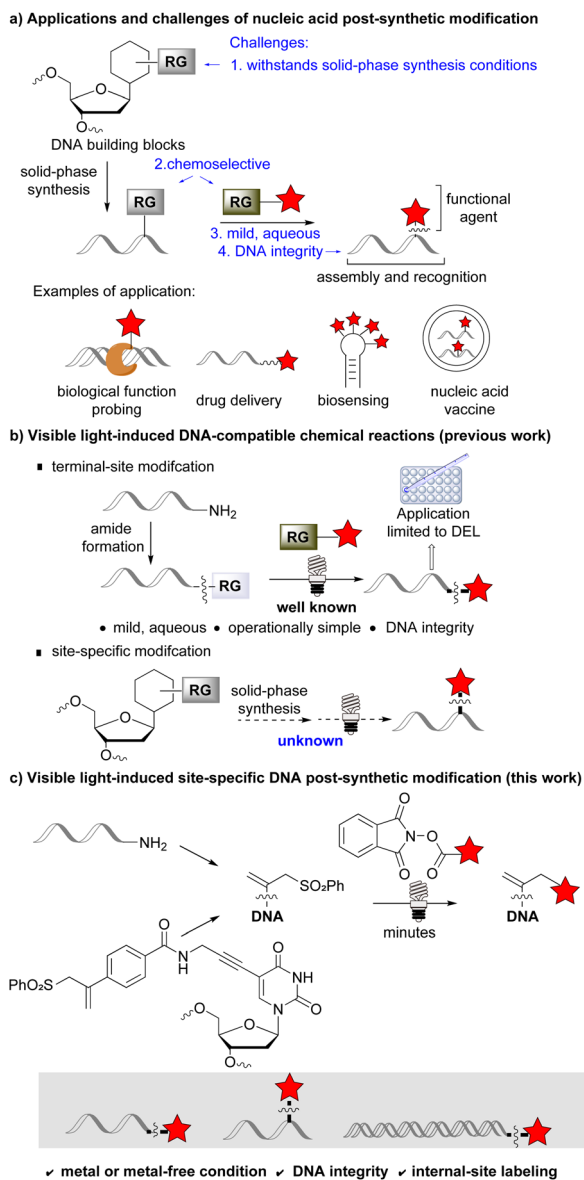
<sup>b</sup>School of Physical Science and Technology, ShanghaiTech University, 100 Haik Road, Shanghai 201210, P. R. China

<sup>c</sup>School of Chemistry and Material Sciences, Hangzhou Institute for Advanced Study, University of Chinese Academy of Sciences, 1 Sub-lane Xiangshan, Hangzhou 310024, P. R. China

†Electronic supplementary information (ESI) available: Complete experimental procedures and full compounds characterization. See DOI: <https://doi.org/10.1039/d4qo00752b>

‡These authors contributed equally.





**Scheme 1** DNA post-synthetic modification via DNA-compatible chemical reactions. RG: reactive group; DEL: DNA-encoded library.

on DNA *via* simple light irradiation while maintaining DNA integrity. However, these photochemical transformations typically start with DNA containing a terminal amino group to introduce one reactive group, which is unsuitable for achieving site-specific nucleic acid modification at arbitrary desired positions (Scheme 1b). Although light control of DNA structure and function aids in spatiotemporal probing of cellular events, the current photochemical toolboxes for site-specific nucleic acid post-synthetic modification primarily rely on ultraviolet (UV) light.<sup>9</sup> We hypothesize that carefully choosing reactive functional groups and exploring photocatalytic reactions could facilitate site-specific DNA post-synthetic modification at any desired position under safe and convenient visible light irradiation.

Allyl sulfone is highly valued in radical allylations, primarily owing to its ease of synthesis and versatile reactivity.<sup>10</sup> Moreover, it exhibits chemical stability even under harsh conditions such as strong acids, bases, and oxidizing agents.<sup>11</sup> Our group and others have previously validated using allyl sulfone as a radical acceptor in various visible light-induced photocatalysis, including 1,2-hydrogen migration, 1,5-hydrogen migration, cascade cyclization, polarity reversal,  $\beta$ -scission, and more.<sup>12</sup> Particularly, we presented the visible-light-induced decarboxylative allylation in neutral aqueous solutions *via* allyl sulfone and *N*-acyloxyphthalimide, resulting in the formation of the allylation adduct.<sup>13</sup> This reaction completes rapidly at room temperature, demonstrating remarkable chemoselectivity within minutes. We envision incorporating allyl sulfone onto nucleobases for on-DNA photocatalytic reactions may offer new possibilities and advantages in advancing photochemical toolboxes for DNA functionalization. Herein, we present site-specific DNA post-synthetic modification at any desired position *via* fast photocatalytic allylation (Scheme 1c). Allyl sulfone groups were introduced into DNA, not only at the terminal site *via* traditional amide formation but also at any desired position including internal and terminal sites through DNA solid-phase synthesis. This visible light-induced on-DNA photocatalytic decarboxylative allylation proceeds rapidly under mild conditions and exhibits excellent chemoselectivity and compatibility with various functional groups along with retaining DNA integrity. The choice of organic photocatalyst also enables metal-free transformation on DNA. Specifically, the introduction of allyl sulfone into DNA *via* solid-phase synthesis enables efficient DNA modification on chemically synthesized single-stranded DNA (ssDNA) at internal and terminal positions, hybridized double-stranded DNA (dsDNA), as well as enzymatically amplified long-chain DNA under visible light.

## Results and discussion

Inspired by our pioneering work on visible light-induced rapid, biocompatible decarboxylative allylation with allyl sulfones,<sup>13,14</sup> we first investigated the feasibility of applying this photochemical reaction on DNA. The direct incorporation of allyl sulfone scaffolds onto DNA was achieved in a single step *via* traditional protocols of amide formation with 20 mer ssDNA C6 NH<sub>2</sub> (Fig. S1<sup>†</sup>). We explored ssDNA-conjugated aryl-substituted allyl sulfone **DNA 1** as the radical acceptor and *N*-acyloxyphthalimide derivative **1a** as the radical precursor for on-DNA photocatalytic coupling under blue LED light (468 nm) irradiation (Table 1, Fig. S2, S3, and S8<sup>†</sup>).<sup>15</sup> Under mild photoirradiation, no damage to DNA was observed (Fig. S4a<sup>†</sup>), and the desired C-allylation product **DNA 2a** was successfully obtained with photocatalyst Ru(bpy)<sub>3</sub>Cl<sub>2</sub> and reductant ascorbic acid (VcH). The on-DNA coupling proceeded rapidly, yielding 79% after a five-minute light irradiation; further irradiation for extended periods did not lead to a significant increase in yield (entries 1 and 2, and Table S1<sup>†</sup>).<sup>16</sup> Lower conversion was observed when employing



**Table 1** Condition screening for the on-DNA photoredox decarboxylative allylation

Entry <sup>d</sup>	Deviation from the standard conditions	Yield <sup>e</sup>
1	None	79%
2	3 h	80%
3	N <sub>2</sub>	75%
4	2000 equiv. <b>1a</b>	73%
5	500 equiv. <b>1a</b>	58%
6	300 equiv. <b>1a</b> <sup>d</sup>	73%
7	VcNa instead of VcH	53%
8 <sup>b</sup>	HE, DIPEA, HCOOH instead of VcH	50%
9	No reductant	0%
10	No light	0%
11	No Ru(bpy) <sub>3</sub> Cl <sub>2</sub>	0%
12	instead of DNA 1	0%

<sup>a</sup> Reaction conditions: **DNA 1** (1 nmol, 1 equiv.), **1a** (1 μmol, 1000 equiv.), ascorbic acid (VcH, 5 μmol, 5000 equiv.), Ru(bpy)<sub>3</sub>Cl<sub>2</sub> (10 nmol, 10 equiv.), pH 7.4 0.5 M Tris buffer/DMF (1:1) (100 μL) with two blue LED (4 W, 468 nm) irradiation at 25 °C for 5 min. <sup>b</sup> HE (Hantzsch ester, 1 μmol, 1000 equiv.), DIPEA (1 μmol, 1000 equiv.), HCOOH (1 μmol, 1000 equiv.). <sup>c</sup> Yields were determined by LC-MS analysis. <sup>d</sup> Reaction was carried out with **DNA 1** (1 nmol, 1 equiv.) **1a** (0.3 μmol, 300 equiv.) in pH 7.4 0.5 M Tris buffer/DMF (1:1) (10 μL) under standard condition.

iridium complexes, such as Ir(dtbbpy)(ppy)<sub>2</sub>PF<sub>6</sub> or fac-Ir(ppy)<sub>3</sub> as the photocatalysts (Table S2†). Notably, this photoredox reaction efficiently occurred under both nitrogen atmosphere and open-air conditions (entry 3). A high amount of **1a** (1000 equiv.) was utilized for rapid and high-yield on-DNA reactions with diluted DNA (10 μM) (entries 1, 4, and 5). Alternatively, reducing the loading of **1a** (300 equiv.) with higher concentration DNA (100 μM) gave comparable yields of desired products (entry 6). The presence of reductants was crucial for the reactions (entries 7–9). Employing sodium ascorbate (VcNa) or Hantzsch ester (HE) as the reductant also facilitated on-DNA coupling with **1a**, albeit with a slightly decreased yield.<sup>17</sup> In contrast, the photo-induced reaction without reductants showed no conversion. Utilizing a 50% aqueous buffer optimized the reaction by efficiently solubilizing both the DNA and *N*-acyloxyphthalimide derivative (Table S4†).<sup>18</sup> Additionally, reactions proceeded smoothly in the presence of cell culture media (DMEM, HEPES), suggesting potential for further utilization in biological systems (Table S5†). As expected, the absence of light and photocatalysts led to no product generation (entries 10 and 11). No reaction occurred when replacing **DNA 1** with allyl sulfone-free DNA, implying the inertness of coupling reactions to DNA without allyl sulfone (entry 12).

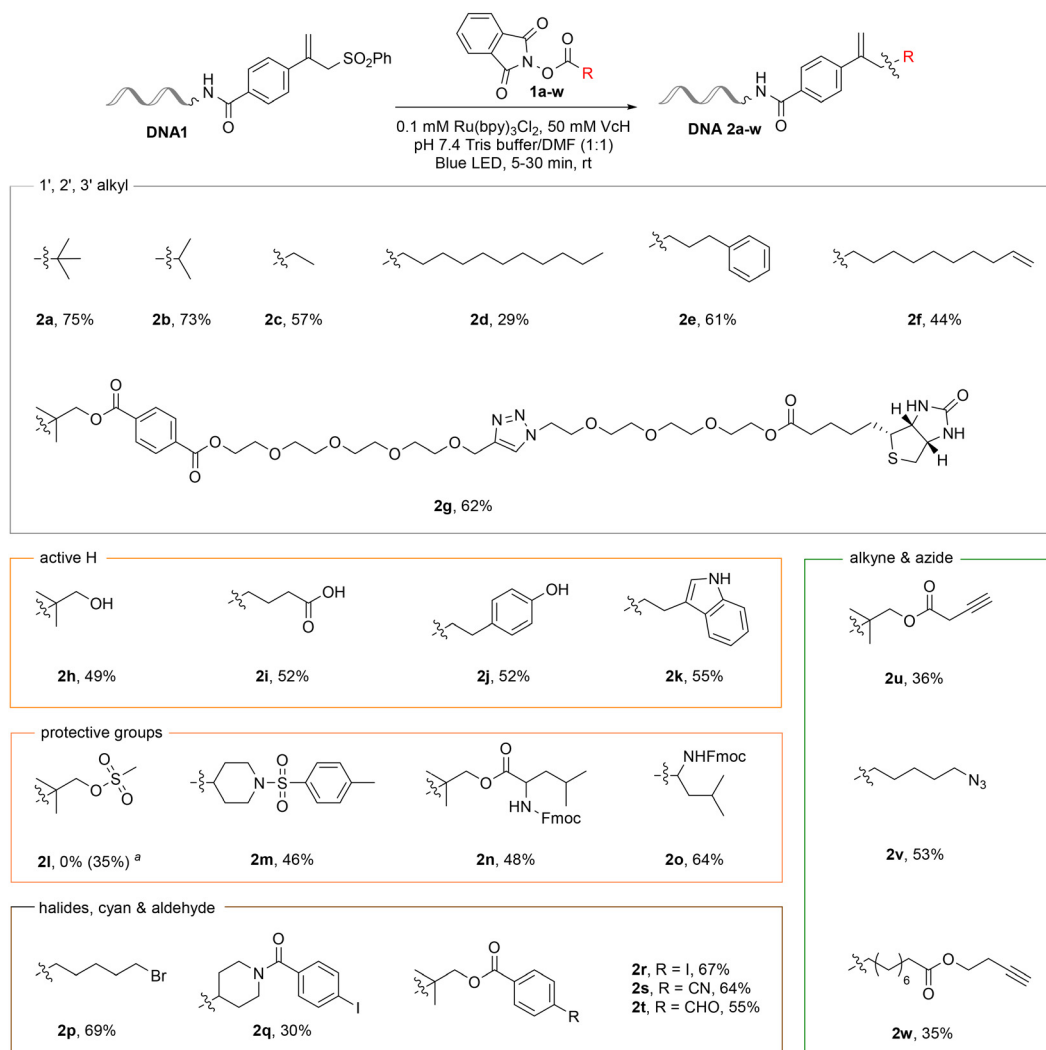
With established favorable reaction conditions, we explored the substrate scope and functional tolerance of

*N*-acyloxyphthalimides **1** (Scheme 2). Encouragingly, the reactions proceeded smoothly with diverse *N*-acyloxyphthalimides bearing primary, secondary, and tertiary alkyl groups (products **DNA 2a–2g**, Fig. S9–S15†). The tertiary alkyl substrates were more reactive, leading to desired coupling adducts in satisfactory yields within 5 minutes. In contrast, the primary and secondary alkyl substrates required extended light irradiation of 30 minutes to achieve comparable yields.<sup>19</sup> To evaluate the functional groups' tolerance of the reaction, we tested substrates containing active hydrogen including unprotected alcohol, carboxylic acid, phenol, and indole. Pleasingly, the presence of these functional groups did not impact the reaction outcomes (products **DNA 2h–2k**, Fig. S16–S19†). When utilizing *N*-acyloxyphthalimides-bearing free carboxylic acids as the radical precursor, a yield of 52% was obtained for product **DNA 2i** (Fig. S17†). The commonly employed protecting groups remained intact during the coupling reaction (products **DNA 2l–2o**, Fig. S20–S23†), except for the mesyl protective group (product **DNA 2l**, Fig. S20†). Furthermore, traditional alkyl radical precursors such as alkyl bromide successfully afforded the desired product **DNA 2p** yielding 69% (Fig. S24†). The reduced yield of **DNA 2q** might be attributed to the limited solubility of *N*-acyloxyphthalimides derivatives **1q** (Fig. S25†). Both transition-metal-sensitive aryl iodide and reduction-sensitive aldehyde and nitrile were well tolerated under the reaction conditions, affording the corresponding products with acceptable yields (products **DNA 2r–2t**, 55% to 67%, Fig. S26–S28†). Moreover, substrates containing alkyne and azide, which could be further diversified on-DNA, were also well-tolerated in the coupling reaction (products **DNA 2u–2w**, Fig. S29–S31†).

The cost and toxicity of transition metal, along with the difficulties in removing metal residues from final products, have motivated ongoing efforts to develop metal-free organic transformation on DNA.<sup>4a,20</sup> We investigated the organic photocatalyst for on-DNA photocatalytic decarboxylative allylation. Pleasingly, Eosin Y with a redox potential similar to Ru(bpy)<sub>3</sub>Cl<sub>2</sub>, enabled on-DNA coupling with **1a**, yielding 80% of **DNA 2a** after 5 minutes of visible light irradiation (Table S2,† entry 4). In contrast, other organic photocatalysts with higher oxidation potential, such as 4CzIPN, Acr-Mes<sup>+</sup>ClO<sub>4</sub><sup>-</sup>, and Ph-Acr-Mes<sup>+</sup>BF<sub>4</sub><sup>-</sup> did not yield any product (Table S2,† entries 5–7). Using Eosin Y with **1g** efficiently formed **DNA 2g** similar to metal photocatalysts (Fig. S5†). Eosin Y proved to be a viable alternative, enabling fast, metal-free on-DNA transformation *via* visible light.

To evaluate DNA integrity after photocatalytic decarboxylative allylation, we quantified the DNA-conjugate product **DNA 2o** using quantitative polymerase chain reaction (qPCR) and elongated it through enzymatic ligation (Scheme 3a, Tables S6 and S7†). In the qPCR analysis, minor differences in DNA amplification efficiency were observed between the standard samples and **DNA 2o**, suggesting the preservation of DNA integrity (Scheme 3b). In the enzymatic ligation experiment, we first hybridized ssDNA tag **DNA 2o** with its complementary ssDNA tag **DNA 3**, forming dsDNA tag **DNA 4**. Subsequent





**Scheme 2** Substrate scopes of *N*-acyloxyphthalimide **1**. Yields were determined by LC-MS analysis. <sup>a</sup> Yield is for the product without a mesyl protective group.

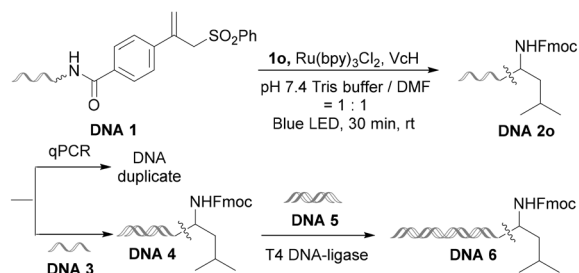
enzymatic ligation efficiently extended **DNA 4** to yield **DNA 6**, incorporating additional 25 bp from **DNA 5** as confirmed by agarose gel analysis and denaturing-PAGE gel analysis (Scheme 3c). These results highlighted the mildness of photocatalytic decarboxylative allylation in retaining the DNA integrity.

Encouraged by the satisfying on-DNA conversion, we proceed to attach the allyl sulfone group onto DNA at both internal and terminal positions through solid-phase DNA synthesis. To evaluate the compatibility of allyl sulfone with solid-phase DNA synthesis conditions, we subjected aryl-substituted allyl sulfone to incubation with strong acids (100 eq. Cl<sub>3</sub>CCOOH), strong bases (NH<sub>4</sub>OH), and strong oxidative conditions (I<sub>2</sub>). Pleasingly, allyl sulfone maintained its integrity after 2 hours of incubation. The synthesis of DNA building blocks bearing allyl sulfone was subsequently started with 5-(3''-aminopropynyl)-2'-deoxyuridine **3** and carboxylic acid-substituted allyl sulfone **2** as the precursors. The allyl sulfone

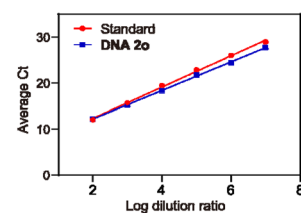
group was linked to the aminopropynyl group of the nucleoside with the peptide coupling reagent HATU to yield intermediate **4** and then converted into DNA building block **5** by standard procedures (Scheme 4a, see the ESI† for details).<sup>21</sup> The chemically synthesized single-stranded DNA, **DNA7** bearing allyl sulfone at internal positions, and **DNA 8** bearing allyl sulfone at terminal positions, were synthesized from this DNA building block by automated solid-phase chemistry and confirmed by LC-MS analysis (Scheme 4a, Fig. S6, S32 and S33†).

We next conducted light-induced post-synthetic modification of **DNA 7**, **8**, and **9** with *N*-acyloxyphthalimides **1** under standard reaction conditions (Scheme 4b, Table S8†). Pleasingly, allyl sulfone at the internal positions of DNA reacted smoothly with *N*-acyloxyphthalimides bearing primary, secondary, and tertiary alkyl groups (**1a**, **1b**, **1g**, and **1v**), yielding **DNA 10** with moderate to good yields (57%–84%, Scheme 4b, Fig. S34–S37†). Similarly, the on-DNA photo-

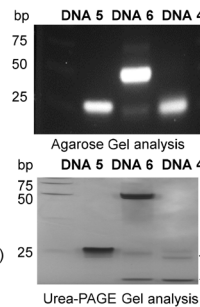


a) Schematic illustration of the qPCR quantification and enzymatic ligation<sup>a</sup>

## b) Values for qPCR assay evaluation



## c) In-gel analysis of ligation reactions



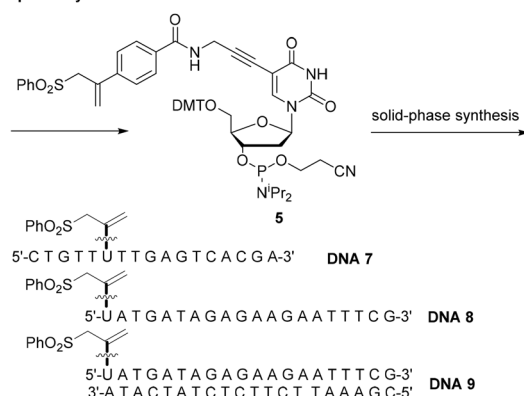
**Scheme 3** DNA integrity assessment. <sup>a</sup> For qPCR quantification, the length of ssDNA prepared in DNA 1 was 108 mer. As for enzymatic ligation, DNA 1 was 20 mer. <sup>b</sup> A DNA conjugate without any chemical transformation served as the standard control.

catalytic transformations proceeded effectively with solid-phase synthesized DNA bearing terminal allyl sulfone modification, resulting in the formation of DNA 11 upon modifying DNA 8 (50%–82%, Fig. S38–S41<sup>†</sup>). It was found that the solid-phase synthesized DNA exhibited comparable reactivity to terminal-modified DNA synthesized *via* traditional amidation coupling, highlighting the effectiveness of the arbitrary site modification *via* fast photocatalytic allylation.

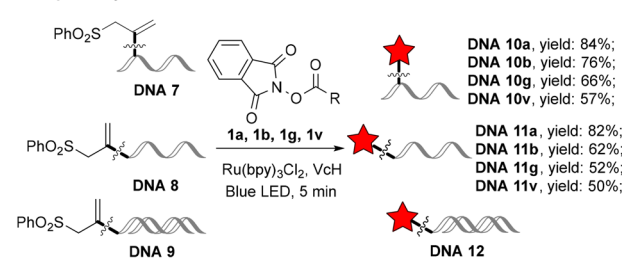
The on-DNA photocatalytic transformations with **1g** increased oligonucleotide fragments weight, detectable through gel electrophoresis. After a 5-minute blue LED irradiation, new bands with higher weight appeared on agarose gel analysis, indicating the formation of modification products DNA 10g and DNA 11g (Fig. S7a,† left panel and right panel). No modification was observed when *N*-acyloxyphthalimide was incubated without light irradiation, whereas a 5-second exposure to blue LED light yielded over 20% modification products during the photocatalytic modification of DNA 7 (Fig. S7b<sup>†</sup>). Further extending the irradiation time led to an increased yield of modification products, demonstrating the dose-dependency of the light irradiation. To investigate the photochemical transformation of dsDNA, allyl sulfone-modified double-stranded DNA 9 was obtained by hybridizing DNA 8 with its complementary DNA strand. Upon light irradiation with **1g**, effective biotin modification on DNA 9 occurred, as confirmed by LC-MS analysis and the urea-PAGE analysis (Fig. S7a, right panel and Fig. S42<sup>†</sup>). These results further confirmed the visible-light-induced DNA modification at both terminal and internal positions in both ssDNA

## DNA

## a) Chemically synthesized single-stranded DNA bearing allyl sulfone via DNA solid-phase synthesis

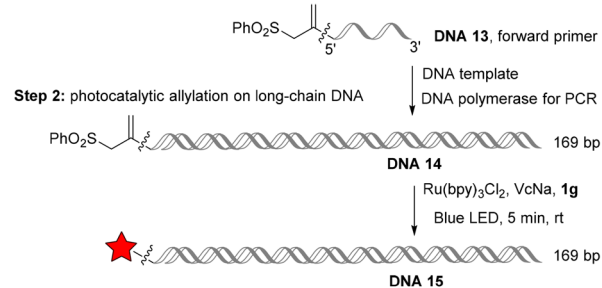


## b) Visible light-induced site-specific DNA post-synthetic modification on various solid-phase synthesized DNA



## c) Visible light-induced site-specific DNA post-synthetic modification on long-chain DNA

Step 1: enzymatically amplify DNA using allyl sulfone-modified primer

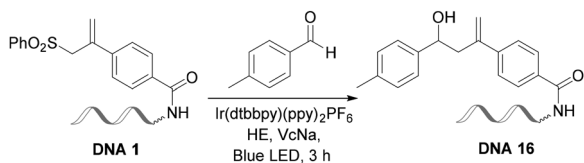


**Scheme 4** Visible-light induced site-specific DNA post-synthetic modification *via* fast photocatalytic allylation.

and dsDNA through fast photocatalytic decarboxylative allylation, representing a rare instance of visible-light-induced site-specific DNA post-synthetic modification.

Post-synthetic modification of nucleic acids is especially valuable for biomacromolecules that are difficult to access through chemical synthesis.<sup>22</sup> To assess the method's effectiveness, we designed and synthesized allyl sulfone-modified forward primer (DNA 13) through DNA solid-phase synthesis (Fig. S43<sup>†</sup>). These primers were then used in a subsequent polymerase chain reaction (PCR) to efficiently amplify a 169 bp double-stranded DNA template (Scheme 4b, Table S9<sup>†</sup>). The allyl sulfone-modified primer has been verified to be compatible with PCR conditions. A clean PCR product, DNA 14, containing allyl sulfone groups at the end of a double-long chain, was obtained and confirmed by agarose gel analysis





**Scheme 5** Visible-light induced on-DNA transformation *via* photocatalytic polarity-inversion with DNA-conjugated allyl sulfone.

(Fig. S7c†). We conducted light-induced photocatalytic transformation on **DNA 14** with **1g** under blue LED irradiation. After 5 min irradiation, the reaction mixture remained as a single bright band in agarose gel analysis, indicating its integrity during light exposure (Fig. S7d†). Remarkably, successful biotin modification of **DNA 14** was achieved, resulting in the production of **DNA 15**, as confirmed by the biotin–streptavidin Southern blot analysis (Fig. S7d†). These results confirm an alternative way for preparing reactive DNA bearing allyl sulfone group through PCR for amplification using modified nucleoside. The visible-light-induced post-synthetic modification method is also suitable for enzymatically amplified long-chain DNA, holding great potential to track DNA replication and translational processes.

Notably, allyl sulfone undergoes various photochemical reactions with different kinds of radical precursors.<sup>12a–d</sup> To further explore the versatility of allyl sulfones in expanding the scope of photochemical reactions in DNA functionalization, we conducted additional photocatalytic transformation using DNA-conjugated allyl sulfone. Remarkably, we successfully achieved polarity-reversed alkylation of aldehydes at 10 μM concentration of **DNA 1** in aqueous solutions (Scheme 5, see the ESI† for details).<sup>12b</sup> Using *p*-methylbenzaldehyde as the radical precursor, this on-DNA photochemical reaction afforded **DNA 16** in yields of 51% when Ir(dtbbpy)(ppy)<sub>2</sub>PF<sub>6</sub> was employed as the catalyst under blue LED irradiation (Fig. S44†).<sup>23</sup> We reasoned that the versatile reactivity of DNA with allyl sulfone enables DNA functionalization *via* diverse photocatalytic transformations.

## Conclusions

In conclusion, we have demonstrated the first visible light-induced site-specific DNA post-synthetic modification *via* fast photocatalytic allylation with allyl sulfone. By utilizing DNA-conjugated aryl-substituted allyl sulfones, we achieved rapid on-DNA alkylation under mild photocatalytic conditions within minutes. This DNA-compatible reaction exhibited excellent chemoselectivity and compatibility with various functional groups along with retaining DNA integrity. Additionally, the use of organic photocatalysts enables metal-free synthetic transformations on DNA. Through DNA solid-phase synthesis, the allyl sulfone groups are incorporated into nucleobases, facilitating DNA modification in chemically synthesized single-

stranded DNA, hybridized double-stranded DNA, and enzymatically amplified long-chain DNA. Moreover, the DNA-bearing allyl sulfone groups facilitated on-DNA photocatalytic polarity reversal reaction, expanding bioorthogonal chemical toolboxes for DNA post-synthetic modification *via* diverse photocatalytic methods.

## Conflicts of interest

There are no conflicts to declare.

## Acknowledgements

Financial support was provided by the National Natural Science Foundation of China 22337005, 22277133, 91753126, Youth Innovation Promotion Association CAS 2023266, CAS Interdisciplinary Innovation Team JCTD-2020-16, Program of Shanghai Academic/Technology Research Leader 21XD1424700, International Partnership Program of the Chinese Academy of Science 033GJHZ2023006FN.

## References

- (a) A. M. Femino, F. S. Fay, K. Fogarty and R. H. Singer, Visualization of Single RNA Transcripts in Situ, *Science*, 1998, **280**, 585–590; (b) M. Schena, D. Shalon, R. W. Davis and P. O. Brown, Quantitative Monitoring of Gene Expression Patterns with a Complementary DNA Microarray, *Science*, 1995, **270**, 467–470; (c) M. O. Loehr and N. W. Luedtke, A Kinetic and Fluorogenic Enhancement Strategy for Labeling of Nucleic Acids, *Angew. Chem., Int. Ed.*, 2022, **61**, e202112931; (d) L. Li, S. Xu, H. Yan, X. Li, H. S. Yazd, X. Li, T. Huang, C. Cui, J. Jiang and W. Tan, Nucleic Acid Aptamers for Molecular Diagnostics and Therapeutics: Advances and Perspectives, *Angew. Chem., Int. Ed.*, 2021, **60**, 2221–2231; (e) S. Ni, H. Yao, L. Wang, J. Lu, F. Jiang, A. Lu and G. Zhang, Chemical Modifications of Nucleic Acid Aptamers for Therapeutic Purposes, *Int. J. Mol. Sci.*, 2017, **18**, 1683–1703; (f) L. M. Larcher, I. L. Pitout, N. P. Keegan, R. N. Veedu and S. Fletcher, DNazymes: Expanding the Potential of Nucleic Acid Therapeutics, *Nucleic Acid Ther.*, 2023, **33**, 178–192; (g) M. Kwak and A. Herrmann, Nucleic acid amphiphiles: synthesis and self-assembled nanostructures, *Chem. Soc. Rev.*, 2011, **40**, 5745–5755.
- K. Karikó, M. Buckstein, H. Ni and D. Weissman, Suppression of RNA Recognition by Toll-like Receptors: The Impact of Nucleoside Modification and the Evolutionary Origin of RNA, *Immunity*, 2005, **23**, 165–175.
- (a) N. Z. Fantoni, A. H. El-Sagheer and T. Brown, A Hitchhiker's Guide to Click-Chemistry with Nucleic Acids, *Chem. Rev.*, 2021, **121**, 7122–7154; (b) A. H. El-Sagheer and T. Brown, Click chemistry with DNA, *Chem. Soc. Rev.*, 2010,



- 39, 1388–1405; (c) L. K. McKenzie, R. El-Khoury, J. D. Thorpe, M. J. Damha and M. Hollenstein, Recent progress in non-native nucleic acid modifications, *Chem. Soc. Rev.*, 2021, **50**, 5126–5164.
- 4 (a) K. Krell, D. Harijan, D. Ganz, L. Doll and H.-A. Wagenknecht, Postsynthetic Modifications of DNA and RNA by Means of Copper-Free Cycloadditions as Bioorthogonal Reactions, *Bioconjugate Chem.*, 2020, **31**, 990–1011; (b) I. Ivancová, D.-L. Leone and M. Hocek, Reactive modifications of DNA nucleobases for labelling, bioconjugations, and cross-linking, *Curr. Opin. Chem. Biol.*, 2019, **52**, 136–144.
- 5 V. Amarnath and A. D. Broom, Chemical synthesis of oligonucleotides, *Chem. Rev.*, 1977, **77**, 183–217.
- 6 (a) B. Matsuo, A. Granados, G. Levitre and G. A. Molander, Photochemical Methods Applied to DNA Encoded Library (DEL) Synthesis, *Acc. Chem. Res.*, 2023, **56**, 385–401; (b) B. Koo, H. Yoo, H. J. Choi, M. Kim, C. Kim and K. T. Kim, Visible Light Photochemical Reactions for Nucleic Acid-Based Technologies, *Molecules*, 2021, **26**, 556–579; (c) Y. Chen, A. S. Kamlet, J. B. Steinman and D. R. Liu, A biomolecule-compatible visible-light-induced azide reduction from a DNA-encoded reaction-discovery system, *Nat. Chem.*, 2011, **3**, 146–153; (d) S. Patel, S. O. Badir and G. A. Molander, Developments in Photoredox-Mediated Alkylation for DNA-Encoded Libraries, *Trends Chem.*, 2021, **3**, 161–175.
- 7 C. Hu and Y. Chen, Biomolecule-compatible chemical bond-formation and bond-cleavage reactions induced by visible light, *Tetrahedron Lett.*, 2015, **56**, 884–888.
- 8 Y. Huang, O. Savych, Y. Moroz, Y. Chen and R. A. Goodnow, DNA-Encoded Library Chemistry: Amplification of Chemical Reaction Diversity for the Exploration of Chemical Space, *Aldrichimica Acta*, 2019, **52**, 75–87.
- 9 (a) B. D. Fairbanks, L. J. Macdougall, S. Mavila, J. Sinha, B. E. Kirkpatrick, K. S. Anseth and C. N. Bowman, Photoclick Chemistry: A Bright Idea, *Chem. Rev.*, 2021, **121**, 6915–6990; (b) U. Reisacher, L. Antusch, R. Hofsäß, C. Schwechheimer, B. Lehmann and H.-A. Wagenknecht, Light-induced functions in DNA, *Curr. Opin. Chem. Biol.*, 2017, **40**, 119–126; (c) A. Tavakoli and J.-H. Min, Photochemical modifications for DNA/RNA oligonucleotides, *RSC Adv.*, 2022, **12**, 6484–6507.
- 10 F. Bertrand, F. L. Guyader, L. Liguori, G. Ouvry, B. Quiclet-Sire, S. StéphanSeguin and S. Z. Zard,  $\alpha$ -Scission of sulfonyl radicals: a versatile process for organic synthesis, *C. R. Acad. Sci., Ser. IIC: Chim.*, 2001, **4**, 547–555.
- 11 (a) A. L. Fuentes de Arriba, F. Urbitsch and D. J. Dixon, Umpolung synthesis of branched  $\alpha$ -functionalized amines from imines via photocatalytic three-component reductive coupling reactions, *Chem. Commun.*, 2016, **52**, 14434–14437; (b) A. Stikute, J. Luginina and M. Turks, Synthesis of allyl sulfones from potassium allyltrifluoroborates, *Tetrahedron Lett.*, 2017, **58**, 2727–2731; (c) F. Xiao, C. Liu, S. Yuan, H. Huang and G.-J. Deng, A Four-Component Reaction for the Synthesis of  $\beta$ -Quinoline Allylic Sulfones under Iron Catalysis, *J. Org. Chem.*, 2018, **83**, 10420–10429.
- 12 (a) J. Zhang, Y. Li, F. Zhang, C. Hu and Y. Chen, Generation of Alkoxy Radicals by Photoredox Catalysis Enables Selective C(sp<sup>3</sup>)-H Functionalization under Mild Reaction Conditions, *Angew. Chem., Int. Ed.*, 2016, **55**, 1872–1875; (b) L. Qi and Y. Chen, Polarity-Reversed Allylations of Aldehydes, Ketones, and Imines Enabled by Hantzsch Ester in Photoredox Catalysis, *Angew. Chem., Int. Ed.*, 2016, **55**, 13312–13315; (c) J. Zhang, Y. Li, R. Xu and Y. Chen, Donor-Acceptor Complex Enables Alkoxy Radical Generation for Metal-Free C(sp<sup>3</sup>)-C(sp<sup>3</sup>) Cleavage and Allylation/Alkenylation, *Angew. Chem., Int. Ed.*, 2017, **56**, 12619–12623; (d) Y. Zhang, Y. Zhang, C. Ye, X. Qi, L. Z. Wu and X. Shen, Cascade cyclization of alkene-tethered acylsilanes and allylic sulfones enabled by unproductive energy transfer photocatalysis, *Nat. Commun.*, 2022, **13**, 6111–6121; (e) D. Liu, J. Zhang and Y. Chen, Investigations on the 1,2-Hydrogen Atom Transfer Reactivity of Alkoxy Radicals under Visible-Light-Induced Reaction Conditions, *Synlett*, 2021, 356–361.
- 13 C. Hu and Y. Chen, Chemoselective and fast decarboxylative allylation by photoredox catalysis under mild conditions, *Org. Chem. Front.*, 2015, **2**, 1352–1355.
- 14 J. Yang, J. Zhang, L. Qi, C. Hu and Y. Chen, Visible-light-induced chemoselective reductive decarboxylative alkynylation under biomolecule-compatible conditions, *Chem. Commun.*, 2015, **51**, 5275–5278.
- 15 We chose DNA 1 as the model substrate for its ease in obtaining >95% purity via HPLC separation. The ssDNA-conjugated allyl sulfone without phenyl substitution is compatible with photoredox decarboxylative allylation, producing the desired allylation products with slightly reduced yields.
- 16 **1a** remained almost stable in the reaction mixture for 30 minutes, with only 9% degradation observed by HPLC analysis (Fig. S4b†). The incomplete DNA conversion may be due to low conversion with a small DNA amount.
- 17 The addition of VcH and VcNa slightly changes the pH of the reaction mixture. VcH provides a slightly acidic environment, which is more favorable for activating the *N*-acyloxyphthalimide derivative substrate. See ref. K. Okada, K. Okamoto and M. Oda, A new and practical method of decarboxylation: photosensitized decarboxylation of *N*-acyloxyphthalimides via electron-transfer mechanism, *J. Am. Chem. Soc.*, 1988, **110**, 8736–8738; G. Kachkovskiy, C. Faderl and O. Reiser, Visible Light-Mediated Synthesis of (Spiro)annelated Furans, *Adv. Synth. Catal.*, 2013, **355**, 2240–2248.
- 18 An aqueous buffer was tested to stabilize the reaction mixture at a neutral pH after adding ascorbic acid. Various aqueous buffers (such as Tris-HCl, PBS, and PB) proved minimal impact on the reaction reactivity (Table S3†).
- 19 This could be attributed to the faster generation of the anion radical from tertiary alkyl substrates during photocatalysis compared to primary and secondary substrates,



which serve as the rate-limiting step in the visible-light-induced decarboxylative allylation. See ref. 17.

- 20 (a) M. Merkel, K. Peewasan, S. Arndt, D. Ploschik and H.-A. Wagenknecht, Copper-Free Postsynthetic Labeling of Nucleic Acids by Means of Bioorthogonal Reactions, *ChemBioChem*, 2015, **16**, 1541–1553; (b) S. R. N. Kolu and M. Nappi, Metal-free deoxygenative coupling of alcohol-derived benzoates and pyridines for small molecules and DNA-encoded libraries synthesis, *Chem. Sci.*, 2022, **13**, 6982–6989.
- 21 J. J. Turner, N. J. Meeuwenoord, A. Rood, P. Borst, G. A. van der Marel and J. H. van Boom, Reinvestigation into the Synthesis of Oligonucleotides Containing 5-( $\beta$ -D-Glucopyranosyloxymethyl)-2'-deoxyuridine, *Eur. J. Org. Chem.*, 2003, 3832–3839.
- 22 M. Hocek, Enzymatic Synthesis of Base-Functionalized Nucleic Acids for Sensing, Cross-linking, and Modulation of Protein–DNA Binding and Transcription, *Acc. Chem. Res.*, 2019, **52**, 1730–1737.
- 23 The on-DNA photocatalytic polarity-reversed alkylation produced **DNA 16** at a yield of 14% using Ru(bpy)<sub>3</sub>Cl<sub>2</sub> catalyst. The increased reactivity of Ir(dtbbpy)(ppy)<sub>2</sub>PF<sub>6</sub> catalyst may be attributed to its stronger reduction ability ( $E^{\circ 1/2\text{III}/\text{II}} = -1.51$  V vs. SCE in MeCN) compared to Ru(bpy)<sub>3</sub>Cl<sub>2</sub> ( $E^{\circ 1/2\text{II}/\text{I}} = -1.33$  V vs. SCE in MeCN).

